

Fast identification of foodborne pathogenic viruses using continuous-flow reverse transcription-PCR with fluorescence detection

Yuyuan Li · Chunsun Zhang · Da Xing

Received: 22 April 2010 / Accepted: 9 July 2010 / Published online: 28 July 2010
© Springer-Verlag 2010

Abstract Being beneficial from dramatic process in biochemical and micro-electro-mechanical technologies, this study presents an integrated microfluidic system capable of performing a continuous-flow reverse transcription-polymerase chain reaction (RT-PCR) combined with fluorescence microscopy for rapid diagnosis of RNA-based viruses. The device consists of two heated cylinders for heating the different reaction zones of the reverse transcription and the amplification. In the amplification cylinder, bath refrigerating is used for thermal protection of the annealing region, which is heated possibly due to the thermal effects of radiation, conduction, and/or convection from denaturation and extension regions, thus resulting in a space-saving design of the whole device. Detection of the amplified products is performed on-line by a fluorescence microscopy with SybrGreen I, a widely used intercalating dye. In this article, the proposed miniature RT-PCR system is used to amplify and detect two RNA-based viruses (Noroviruses (NVs) and Rotaviruses (RVs)), which are now recognized as the most common etiological agents of acute viral gastroenteritis causing numerous outbreaks worldwide. The experimental data have demonstrated the ability of the presented system to perform a two-step or one-step RT-PCR process. On this device, the NVs and RVs RNA samples were successfully reverse transcribed and amplified within 1 h, and the limit of detection of the

RNA concentration was 6.4×10^4 copies μl^{-1} using one-step RT-PCR process. Consequently, the developed microfluidic system can provide a promising platform for fast diagnosis of RNA-based viruses.

Keywords Continuous-flow · Reverse transcription · Polymerase chain reaction · Microfluidics · On-line fluorescence detection · Foodborne pathogen

1 Introduction

The past decade has witnessed many significant advances in molecular biology and nucleic acid analysis technology, particularly in the genomics and diagnosis fields. The polymerase chain reaction (PCR) technology for DNA amplification was first reported by Kary Mullis (Saiki et al. 1985), which has been applied to a diverse range of basic research and application fields. Recently, attention has focused on developing microfluidic-based PCR devices (Nakano et al. 1994; Northrup et al. 1993), since they offer lower thermal capacitance for rapid thermal cycling (Hoang et al. 2008), reduced analysis-times, low consumption of sample/reagent, portability, and the potential for high automation and integration of various analytical procedures (Obeid and Christopoulos 2004; Prakash et al. 2008b). Generally, microfluidic PCR devices can be divided into two formats (Zhang et al. 2006; Zhang et al. 2007; Zhang and Xing 2007): microchamber stationary PCR (Beer et al. 2007; Belgrader et al. 2003; Ottesen et al. 2006; Prakash and Kaler 2007), which can achieve PCR functions by adjusting temperature cycling in a stationary microchamber, and continuous-flow PCR (Dorfman et al. 2005; Kiss et al. 2008; Kopp et al. 1998; Park et al. 2003; Wang et al. 2009), in which the reaction mixture moves through

Y. Li · C. Zhang (✉) · D. Xing (✉)
MOE Key Laboratory of Laser Life Science and Institute
of Laser Life Science, College of Biophotonics,
South China Normal University, Guangzhou 510631,
People's Republic of China
e-mail: zhangcs@snu.edu.cn

D. Xing
e-mail: xingda@scnu.edu.cn

two or three different temperature regions, thus the thermal cycling is obtained.

While there have been a number of reports of nucleic acid amplification on microdevices for the DNA-based disease diagnosis, however, a lot of diseases do not result from DNA virus but RNA virus, such as Noroviruses (NVs) and Rotaviruses (RVs), which are now recognized as the most common etiological agents of acute viral gastroenteritis causing numerous outbreaks worldwide (Kou et al. 2008). NVs and RVs are usually spread by the fecal–oral route via ingestion of contaminated food or water (Atmar and Estes 2001), by person-to-person transmission (Becker et al. 2000), or by airborne droplets of infected vomitus (Marks et al. 2003). To date, NVs cannot be cultivated from clinical samples, and no animal models are available to study NVs. RVs can be cultured, and however, it is very difficult. The primary methods for NVs or RVs diagnosis were electron microscopy (EM), enzyme-linked immunosorbent assay (ELISA), and reverse transcription-PCR (RT-PCR) (Gouvea et al. 1990; Koopmans et al. 2002; Medici et al. 2005). Due to its high sensitivity and specificity, RT-PCR has become the most sensitive and commonly used method for the detection of these viruses. However, this approach is time-consuming and expensive when standard thermocyclers are used. Therefore, the functional integration of RT and PCR onto a miniaturized RT-PCR device is appealing. Similar to microfluidic PCR devices, the miniaturized RT-PCR devices can also be divided into two categories: microchamber stationary RT-PCR and continuous-flow RT-PCR. A functional lab-on-a-chip for RT-PCR was reported by Liao et al. (2005), where the development of a miniature RT-PCR system was used for the diagnosis of RNA-based viruses. This miniature RT-PCR was performed using a two-step reaction approach (i.e., performing RT and then moving the mixture to another chamber to perform PCR) followed by off-chip detection. Single-step RT-PCR approaches (wherein both RT reaction and PCR are performed in the same reaction chamber with no human intervention between these steps) have been reported recently. Quake and co-workers (Marcus et al. 2006b) were one of the first groups to demonstrate microchip RT-PCR in a single chamber. Although there have been a few demonstrations (Beer et al. 2008; Hsieh et al. 2009; Huang et al. 2006; Kaigala et al. 2008; Lee et al. 2008; Lien et al. 2007; Lien et al. 2009; Marcus et al. 2006a, b; VanDijken et al. 2007) of chamber stationary RT-PCR microfluidics, they generally lack the flexibility to change the reaction rate, resulting in more cycling and heating time. Moreover, in order to reduce the reaction time and power consumption, the system thermal mass often needs to be optimized considerably (Liu et al. 2002). Compared with microchamber stationary system, the continuous-flow system allows for rapid heat

transfer and thermal cycling of the minute fluidic element due to both the high surface-to-volume ratio (SVR) and the short linear thermal diffusion distance in the microfluidic channels. This design advantage is achieved by maintaining the zones at preset constant temperatures (Obeid et al. 2003). Currently, the structural styles of the continuous-flow RT-PCR microfluidics can be divided into two main categories: the serpentine-channel continuous-flow RT-PCR (Felbel et al. 2008; Obeid et al. 2003; Obeid and Christopoulos 2003; Tsai and Sue 2006) and the spiral-channel continuous-flow RT-PCR (Hartung et al. 2009). In the latter configuration, PCR device has an underlying advantage of a circular arrangement of temperature zones in the sequence of denaturation, annealing, and extension, which could increase the PCR efficiency compared with the former. Hartung et al. (2009) have reported a flow-through RT-PCR system for the diagnosis of RNA-based pathogenic viruses. However, this microfluidic device is not very compact, which has a diameter of 7 cm, thus resulting in more energy consumption. In addition, it has not an on-line detection method for the pathogenic virus diagnosis. A miniaturized fluorescence detector has been demonstrated to measure the fluorescence intensity of the single fluid segments inside the reaction tube, where the only SybrGreen I labeled λ -DNAs instead of the pathogenic virus RNAs were used.

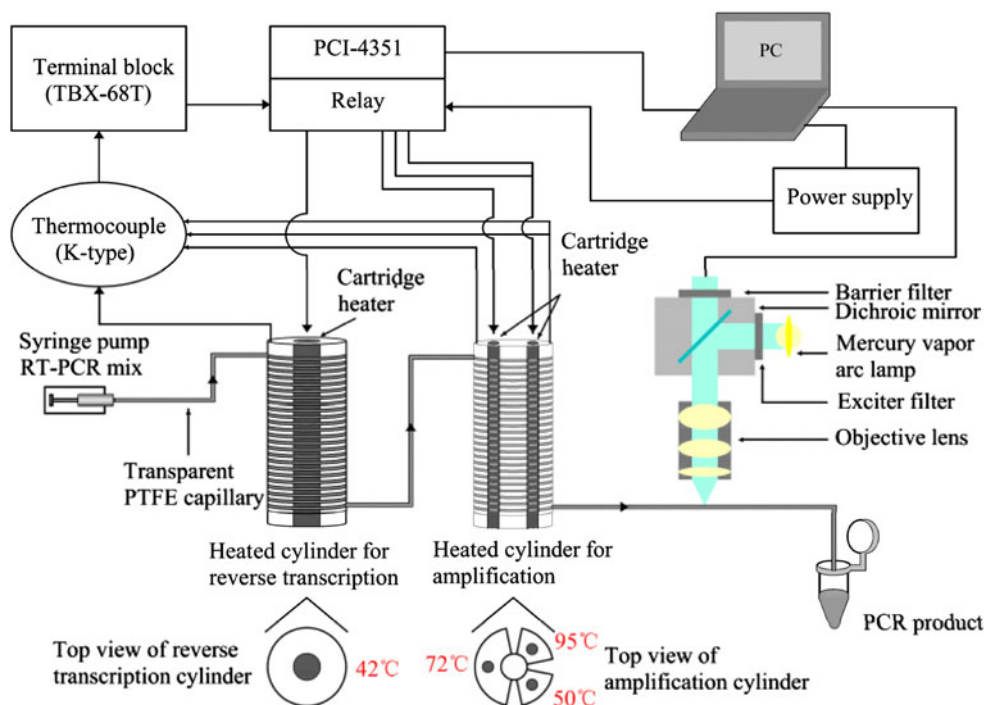
This study presents a compact continuous-flow reverse transcription-PCR (RT-PCR) integrated with fluorescence detection for rapid identification of NVs and RVs. The device consists of two heated cylinders for reverse transcription and amplification reactions. In the amplification cylinder, the cycling water bath is utilized for thermal protection of the annealing region which is heated probably due to the effects of heat radiation, conduction, and/or convection from denaturation and extension zones, thus leading to a space-saving design of the whole device. The amplified products are detected on-line by a fluorescence microscopy, in combination with SybrGreen I, a widely used intercalating dye (Trantakis et al. 2010).

2 Materials and methods

2.1 Design of the experimental arrangement

The continuous-flow RT-PCR microfluidic device, depicted schematically in Fig. 1, was manufactured by the Automation Engineering R&M Centre (AERMC), Guangdong Academy of Sciences (Guangzhou, China). It includes one heated cylinder for reverse transcription and another for amplification. The two cylinder reactors both have a diameter of 3.5 cm and a height of 7.5 cm. The RT cylinder includes one larger central hole (12 mm diameter) for the

Fig. 1 Schematic diagram of the continuous-flow reverse transcription-PCR (RT-PCR) thermocycler setup with fluorescence detection. The reactor is controlled with a LabVIEW program



resistance cartridge heater (12 mm diameter, 60 mm length, 100 W, Guangzhou Haoyi Thermal Electronics Factory, Guangzhou, China) and two small holes (1 mm diameter and 10 mm deep) for the K-type thermocouples (K-type, 0.005 inch diameter, Omega Engineering Inc., Stamford, CT, USA). The amplification cylinder is machined into three pieces corresponding to the denaturation, annealing, and extension regions. The extension region is twice the size of the other two zones, thus occupying half the cylinder. The three thermostatic zones are mounted together by bakelite with a ~ 7 mm slit between them in order to avoid a direct thermal contact among the three parts. For thermal protection, a small hole (3.5 mm diameter) was drilled through the annealing region for bath refrigerating, which provides better temperature control and uniformity. Each zone includes one larger central hole (6 mm diameter) for the resistance cartridge heater (6 mm diameter, 60 mm length, 100 W, Guangzhou Haoyi Thermal Electronics Factory, Guangzhou, China) and two small holes (1 mm diameter and 10 mm deep) for the K-type thermocouples. The thermocouples were connected to a data acquisition system (Model PCI 4351, National Instruments Corp., Austin, TX, USA) that converted the analog signal to a digital one. To control the temperatures for reverse transcription at 42°C, denaturation at 95°C, annealing at 50°C, and extension at 72°C, a computer received the temperature signal through a PCI-4351 interface (National Instruments Corp., Austin, TX, USA) and determined the power input to the heater using a home-made fuzzy proportional/integral/

derivative (PID) control algorithm that was programmed with LabVIEW 8.0 (Version 8.0, National Instrument Corp., Austin, TX, USA).

The two cylinder reactors are connected by a transparent PTFE capillary (i.d. 0.5 mm/o.d. 0.9 mm, Wuxi Xiangjian Tetrafluoroethylene Product Co. Ltd. (Wuxi, China)). A residence time of 45 min can be realized in the RT zone with a capillary length of about 5.5 m when a flow rate of $23.6 \mu\text{L min}^{-1}$ is used. The amplification cylinder can be used for the realization of up to 40 temperature cycles. The length of the capillary amounts about 5 m in case of 40 cycles including the inlet for sample injection and the outlet for product collection. It enters the cylinder through a hole (1.5 mm diameter) crossing the annealing and denaturation zones, thus providing an initial denaturation step. Then the capillary is wound 40 cycles in the spiral channel which is 1.1 mm width and 1.1 mm depth. The capillary exits the cylinder through a hole (1.5 mm diameter) in the elongation region, providing an additional extension on the 40th cycle. The inlet and outlet lengths of the capillary were about 0.2 and 0.6 m, respectively.

In addition to the two cylinder reactors, the experimental arrangement also includes a precision syringe pump (Cole-Parmer® CZ-74901-15, Illinois, USA) for compelling the reaction sample flowing continuously through the microchannel, and a fluorescence microscope (M17, Bio-Rad, CA, USA) for product detection was also integrated in the complete setup (Fig. 2). The filters in the fluorescence microscope were chosen as follows: EF450-490

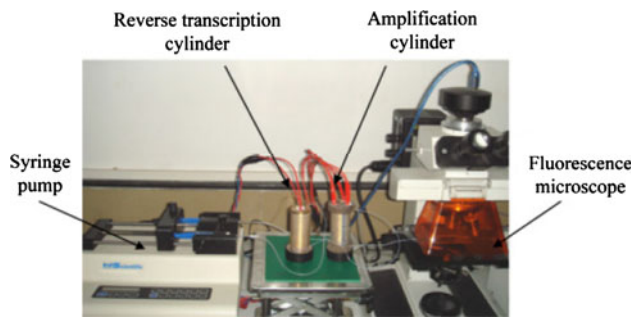


Fig. 2 Photograph of the complete microfluidics system of the continuous-flow reverse transcription-PCR (RT-PCR) thermocycler setup with fluorescence detection, which was used for the described experiments

(BP470), BF520, and DM505. A cooled charge-coupled device (CCD) camera (MC15, Guangzhou Ming-Mei Technology Co., Ltd, Guangzhou, China) was used to acquire pictures of fluorescence in the capillary every few minutes at the end of PCR reaction.

2.2 Reagents and samples

The reaction reagents, 5× M-MLV buffer (375 mM KCl, 250 mM Tris-HCl (pH 8.3), 15 mM MgCl₂, 50 mM DTT), reverse transcriptase M-MLV (RNase H⁻) (200 U μl⁻¹), Ribonuclease inhibitor (40 U μl⁻¹), 10× Taq DNA polymerase buffer (500 mM KCl, 100 mM Tris-HCl (pH 8.3), 15 mM MgCl₂), thermostable Taq polymerase (5 U μl⁻¹) and Deoxynucleotide triphosphate (dNTPs) (2.5 mM each of dATP, dGTP, dCTP, and dTTP) were all purchased from TaKaRa Biotechnology (Dalian) Co., Ltd. The double-deionized (dd) H₂O was offered by Tiangen Biotech Co. Ltd. (Beijing, China). Diethylpyrocarbonate (DEPC) was from Shanghai Sangon Biological Engineering & Technology services Co. Ltd. (SSBE), China. Primers of NVs target the RNA-dependent RNA polymerase gene and can detect GGI and GGII simultaneously. Primers of RVs are designed according to the VP7 gene. The oligonucleotide primers (Kou et al. 2008) (Table 1) were synthesized by Invitrogen Biotechnology Co., Ltd (Shanghai, China). RNA samples of NVs and RVs were gifts from Guangdong provincial center for diseases control and prevention (GDCDC, Guangzhou, China) and Guangzhou overseas

Chinese hospital (The first affiliated hospital of JiNan university, Guangzhou, China).

Bovine serum albumin (BSA) (Fraction V, Purity ≥98%, Biotechnology Grade, No. 735094), which was used to dynamically coat the inner surface to decrease the surface adsorption (Zhang et al. 2006), was purchased from Roche Diagnostics GmbH (Mannheim, Germany). Sodium hypochlorite solution, which was used to remove the residual nucleic acid from the microchannel after each amplification, was from Guanghua Chemical Factory Co. Ltd. (Guangzhou, China). GoldViewTM and SybrGreen I dyes were purchased from SBS Genetech Co. Ltd. (Beijing, China). The DL 2000 DNA markers, which contain 2000, 1000, 750, 500, 250, and 100 bp DNA fragments, were from Win Honor Bioscience (South) Ltd. (Guangzhou, China).

2.3 Modification of the inner surface of capillary

To reduce reaction inhibition and reagent adsorption, the PTFE capillary was cleaned and passivated according to the protocol of our previous work (Li et al. 2009; Wang et al. 2009). Briefly, the PTFE capillary was rinsed with 200 μl 0.5% sodium hypochlorite at the flow rate of 100 μl min⁻¹, and washed with deionized water. The capillary used for RT need to be treated with DEPC water. To further protect the reaction from surface inhibitory effects, the static and dynamic passivation methods were both used for the sacrificial surface adsorption of chemical additives comprising 0.025% BSA. For the static passivation, 200 μl 1× RT or PCR buffer containing 0.025% BSA solution was introduced to the capillary and was driven by a precision syringe pump with the flow rate of 50 μl min⁻¹. For the dynamic passivation, BSA of a certain concentration was added to the RT or PCR mixture.

2.4 Continuous-flow RT protocol

For the detection of the foodborne pathogenic virus diseases, the RT reaction is an essential process to synthesize cDNA from the clinical RNA samples. In the separate continuous-flow RT reactions, the optimum assay was performed in 10 μl of a mixture containing 2 μl target RNA, 1× M-MLV buffer, 0.5 mM of each dNTP, the primer pair (1 μM each), 20 U RNase Inhibitor, 100 U of

Table 1 Primers of NVs and RVs (Kou et al. 2008)

Virus	Primer	Sequence (5′–3′)	Location
NVs (327 bp)	JV12	ATACCACTATGATGCAGATTA	4552–4572
	JV13	TCATCATCACCATAGAAAGAG	4858–4878
RVs (392 bp)	P1	GGCTTTAAAAGAGAGAATTTCCGTCTGG	1–28
	P2	GATCCTGTTGGCCATCC	376–392

M-MLV, and 0.025% (m/V) BSA. The RT mixture was introduced into the capillary from the inlet and compelled by the precision syringe pump to flow continuously through the microchannel. The flow velocity was controlled by the syringe, and a residence time of 45 min could be realized in the RT zone if a flow rate of $23.6 \mu\text{l min}^{-1}$ was used. The flow rate of $35.4 \mu\text{l min}^{-1}$ was also performed, thus the RT process only need 30 min.

To verify the performance of the microfluidic device, the positive-control RT was performed on a conventional PCR apparatus, which was a commercial Mastercycler gradient PCR machine (Eppendorf A G, Hamburg, Germany). Reverse transcription reaction was carried out at 42°C for 60 min followed by 20 min at 75°C to prevent non-specific binding.

2.5 Continuous-flow PCR protocol

Following the RT of the RNA sample, $2 \mu\text{l}$ of the synthesized cDNA was used for the further amplification. For continuous-flow PCR amplification, $25 \mu\text{l}$ of PCR mixture consists of $1\times$ PCR buffer, 0.2 mM of each dNTP, the primer pair (0.4 μM each), SybrGreen I ($1\times$), 0.1 U μl^{-1} Taq DNA polymerase, and 0.025% (m/V) BSA. The PCR mixture was introduced into the capillary from the inlet and driven by the precision syringe pump to flow continuously through the microchannel. The 0.2 ml thin-walled polypropylene tube was used to collect the products and stored at 4°C for further analysis.

In order to verify the rapid detection capability of the microfluidic device, PCR was performed at different flow rates of the corresponding PCR mixture through the thermal-cycling capillary. The flow velocity was controlled by the syringe, which ranged from 23.6 to $117.8 \mu\text{l min}^{-1}$. The components in the PCR mixture were the same as those mentioned above, but cDNA was tenfold diluted. In order to determine the sensitivity of continuous-flow PCR system, tenfold serial dilution of the cDNA was made and the 327 bp sequence of NVs was amplified at a flow rate of $41.2 \mu\text{l min}^{-1}$.

To characterize amplification on the microfluidic device (speed, specificity, and yield), the positive-control PCR was also performed on a conventional PCR apparatus. The cycling procedures were set as follows: an initial step of denaturation at 94°C for 3 min; 40 cycles of denaturation at 94°C for 30 s, annealing at 50°C for 30 s, and elongation at 72°C for 1 min; final extension at 72°C for 3 min. In total, the above cycling program needs 95 min. To validate the amplification process, no-template control reactions were setup with all assay reagents and ddH₂O instead of sample DNA. In this work, all experiments in this work were repeated three times to verify the accuracy of the experiments.

2.6 Continuous-flow RT-PCR protocol

For the one-step continuous-flow RT-PCR, $20 \mu\text{l}$ of reaction mixture consisted of $2 \mu\text{l}$ target RNA (3×10^8 and 6.4×10^7 copies μl^{-1} of NVs and RVs RNA, respectively), $1\times$ PCR buffer, 0.5 mM of each dNTP, the primer pair (0.4 μM each), SybrGreen I ($1\times$), 40 U RNase Inhibitor, 200 U of M-MLV, 0.2 U μl^{-1} Taq DNA polymerase, and 0.025% (m/V) BSA. The reaction mixture flowed continuously through the microchannel using a flow rate of $23.6 \mu\text{l min}^{-1}$ for the RT process and $41.2 \mu\text{l min}^{-1}$ for the PCR process. Characterization of limit of detection (LOD) for the developed system was performed from RVs RNA ranging from 6.4×10^8 to 6.4×10^2 copies μl^{-1} using the same reaction cocktail.

On the conventional PCR apparatus, the reaction mixture was heated to 42°C for 60 min followed by initial denaturation to 94°C for 3 min and then amplified for 40 cycles: 94°C for 30 s, 50°C for 30 s, and 72°C for 1 min. The whole reaction process occupied about 150 min.

2.7 Segmented-flow RT-PCR of different RNA viruses

Reaction mixtures (10 μl) for the one-step segmented-flow RT-PCR were prepared with different RNA viruses and PCR primers for detecting NVs and RVs simultaneously. They were sequentially injected into the reaction capillary. The concentrations of NVs and RVs target RNAs were 3×10^9 and 6.4×10^8 copies μl^{-1} , respectively. The negative controls without RNA viruses were also injected to ascertain whether the resulting amplicon was a product of residual contamination. Then these reaction mixtures flowed continuously through the microchannel using a flow rate of $23.6 \mu\text{l min}^{-1}$ for the RT process and $41.2 \mu\text{l min}^{-1}$ for the PCR process. Between each reaction mixture introduced, we interposed small air gaps, $5 \mu\text{l}$ of $1\times$ PCR buffer containing $0.2\times$ bromophenol blue (BPB) buffer, and then small air gaps. This cleaning method was used to effectively remove the residual RNA and/or DNA from the microchannel, and each RT-PCR product could also be collected separately for further analysis.

2.8 Analysis of amplification products

Combined with continuous-flow RT-PCR, fluorescence intensity detection using SybrGreen I was performed with the fluorescence microscopy. The images were analyzed with the MS 1.0 (Guangzhou Ming-Mei Technology Co., Ltd, Guangzhou, China) software as follows (Liu et al. 2002): in each picture, three circles inside the fluid microchannel were chosen to get an average value of the fluorescence intensity. Similarly, three circles outside the

microchannel were selected to make another average value as the background of this picture. The latter value was subtracted from the former to obtain the fluorescence of the solution inside the fluid microchannel.

After on-line detection, 5 μl of each PCR products with 1 μl 6 \times loading buffer were separated by agarose gel electrophoresis. Loading buffer contained 30 mM EDTA, 36% (v/v) Glycerol, 0.05% (w/v) Xylene Cyernol FF, and 0.05% (w/v) Bromophenol Blue (BPB). The gel was prepared with 1.5% of agarose in 0.5 \times TBE containing 0.5 $\mu\text{l ml}^{-1}$ of GoldViewTM as fluorescence dye. The gel was run for 30 min at a constant voltage of 100 V, and then the amplified fragments were visualized under UV light. The DL 2000 DNA markers, which contain 2000, 1000, 750, 500, 250, and 100 bp DNA fragments, were used as standards for the evaluation of the gels.

3 Results and discussion

3.1 Evaluation of RT and PCR micro-reactors

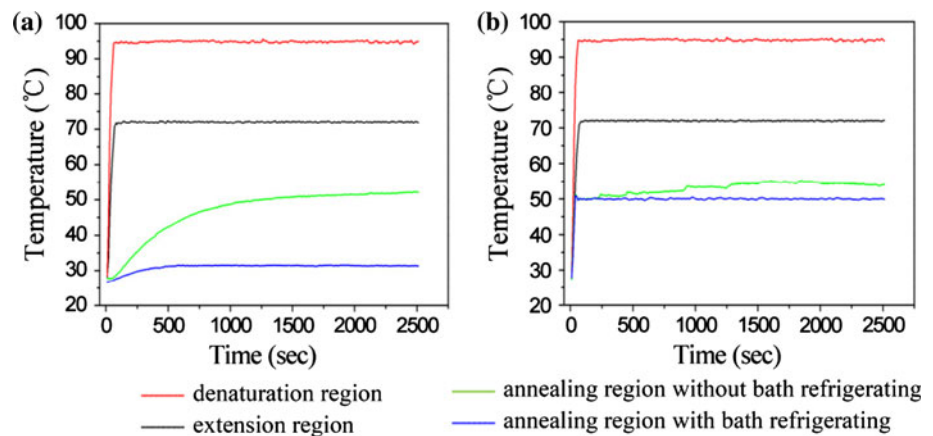
In most of the spiral-channel continuous-flow PCR instruments, it is of particular concern to keep the annealing region to be thermostable. For example, within the Dorfman et al.'s work (2005), the three temperature zones were isolated one from another by thermally insulating sheets, which were affixed between the pieces of the copper cylinder. And a turbine blew ambient air through three flow-through ventilation holes per quarter-cylinder, providing better temperature control and uniformity. Park et al. (2003) brought two adjacent copper blocks to have an air gap of ~ 5 mm between so as to secure thermal insulation. In our previous work, the continuous-flow PCR cylinder was in a diameter of 4 cm, and the three temperature zones were separated from each other by thermally insulating sheets, which had a thickness of 3 mm (Li et al. 2009). Compared with the work reported

previously, the currently developed amplification cylinder is more compact with a diameter of 3.5 cm and even smaller. To avoid a direct thermal contact among the three thermostatic zones, they are mounted together by bakelite with a ~ 7 mm slit between them. In addition, a circulating water bath is used to obtain the steady and uniform annealing temperature. Figure 3 shows the effect of bath refrigerating on the temperature control. When the denaturation and extension zones were heated to 95 and 72 $^{\circ}\text{C}$, respectively, the temperature of the annealing region, which was not heated, gradually rose to 52.5 $^{\circ}\text{C}$ due to cross-talk effects from denaturation and extension regions. However, when the annealing region was refrigerated by the circulating water bath, the temperature could be kept constant at 31 $^{\circ}\text{C}$ (Fig. 3a). In the other words, the annealing temperature of this device could be set at any temperature above 31 $^{\circ}\text{C}$ by using the bath refrigerating. Similarly, when the annealing temperature was set at 50 $^{\circ}\text{C}$ (Fig. 3b), the actual annealing temperature was increased to 54 $^{\circ}\text{C}$ without bath refrigerating, and was kept constant at 50 $^{\circ}\text{C}$ if the annealing zone was cooled by the circulating water bath. Therefore, the bath refrigerating contributes to a better temperature control and uniformity of the developed continuous-flow PCR device.

3.2 Characterization of the continuous-flow PCR amplification

Pursuing high-speed PCR is one of the major motivations in the development of microfluidic PCR. The cycling rate of continuous-flow PCR thermocycler depends, to some extent, on the flow rate of the PCR mixture, the substrate material and the size of the microchannel (Zhang and Xing 2007). Therefore, an obvious characteristic of the continuous-flow PCR amplification is that thermocycling rates of PCR amplification can be regulated by changing the flow rates of the PCR mixture through the flow channel. Figure 4a shows the on-line fluorescence detection results

Fig. 3 Effect of the bath refrigerating on the temperature control and uniformity of the developed continuous-flow PCR device. **a** The annealing region was not heated. **b** The annealing temperature was set at 50 $^{\circ}\text{C}$



of the amplified 327 bp sequence in NVs, which are obtained at flow rates ranging from 23.6 to 117.8 $\mu\text{l min}^{-1}$, whereas Fig. 4b shows the corresponding gel electrophoresis results. It can be seen from Fig. 4 that the phenomena the experimental results shown are similar. With the increase of flow rates within the reaction microchannel, the amount of PCR products is gradually decreased, but the PCR reaction speed is raised gradually. The reason for this behavior might be that the residence time in each region is reduced in case of enhanced process speed. The corresponding time it takes for the PCR mixtures to flow through the PTFE capillary ranges from approximately 45 to 9 min. At a flow rate of 88.3 $\mu\text{l min}^{-1}$, the PCR products can be detected within about 12 min after 40 cycles, where the amplification takes about 10 min (lane 5 in Fig. 4b). This

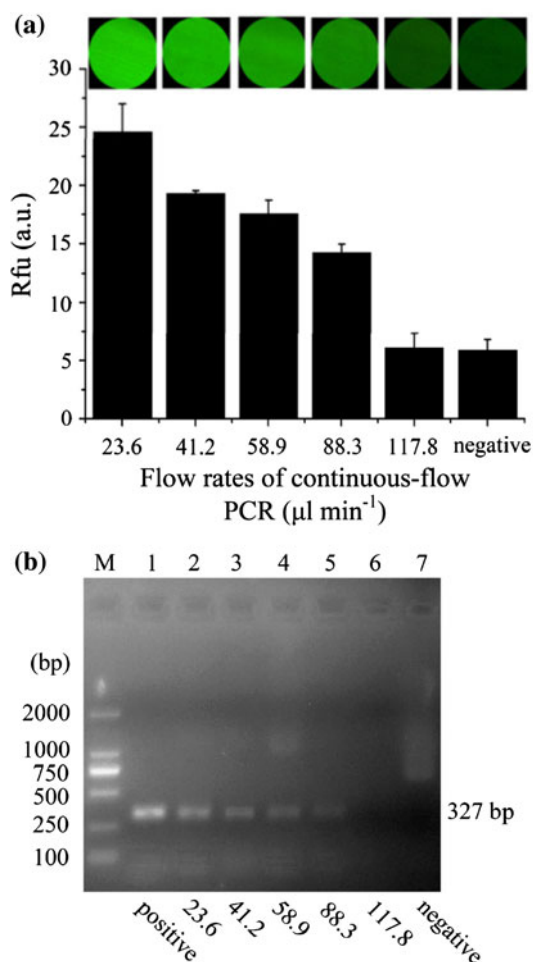


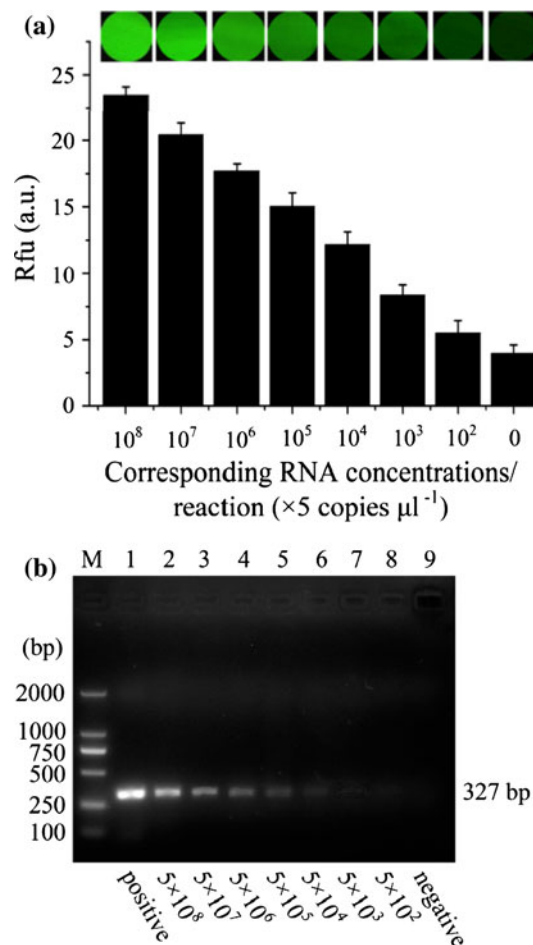
Fig. 4 Effect of the flow rates on the continuous-flow PCR yield. **a** Fluorescence detection of PCR products. **b** Gel electrophoresis analysis of PCR products. Lane M DL 2000 Marker. Lane 1 the positive-control PCR product from the conventional PCR machine (a commercial Mastercycler gradient PCR machine). Lanes 2–6 continuous-flow PCR products at various flow rates of 23.6, 41.2, 58.9, 88.3, and 117.8 $\mu\text{l min}^{-1}$, respectively. Lane 7 the negative-control PCR, PCR mixture solution with no cDNA sample run at the flow rate of 58.9 $\mu\text{l min}^{-1}$

flow rate corresponds to residence times of about 3 s in the denaturation zone, 3 s in the annealing zone and 6 s in the extension zone. Additional 3 s per cycle is consumed by the residence time in the ~ 7 mm slit between three thermostatic zones. It is worth noting that the cycle time is 15 s, which is equivalent to Park et al.'s work (2003), and less than that obtained by other reports (Table 2). In addition, the PCR products cannot be obviously observed when the flow rates were increased to 117.8 $\mu\text{l min}^{-1}$ or higher (lane 6 in Fig. 4b). It could be affected by the size of the PTFE capillary. The thick-walled PTFE capillary with low-thermal conductivity will increase the time required to transfer the heat from the outer to the inner of the capillary, and likewise the large diameter of the capillary will reduce the speed of thermal equilibration of the PCR reaction mixture in the capillary channel. And the thick-walled PTFE capillary may also affect the sensitivity of the fluorescence detection. In addition to the above reasons, we also attribute this to the decreased residence time in the extension zone. Since the extension rate of Taq polymerase is usually 60–100 nucleotides s^{-1} at 72°C in conventional PCR (Zhang and Xing 2010b), an extension time of 6 s is considered sufficient for the 327 bp amplified products. Therefore, when the flow rate was 88.3 $\mu\text{l min}^{-1}$ (the corresponding extension time was slightly more than 6 s) (lane 5 in Fig. 4b), the signal intensity of 327 bp PCR products could still be detected although it was not as strong as those in the case of flow rates of 58.9 $\mu\text{l min}^{-1}$ or smaller.

It is also important to study the effect of the amount of initial cDNA on continuous-flow PCR amplification. As the SVR (8 mm^{-1}) of the capillary channel in the presented continuous-flow PCR microfluidics is great higher than that of commercial PCR reaction tubes (1.5 mm^{-1}) (Li et al. 2009), there is greater possibility of adsorption of biomacromolecules onto the capillary inner surface, such as the Taq enzyme and the DNA molecules, which will inhibit the PCR amplification (Prakash et al. 2008a). Based on our previous work (Li et al. 2009), the concentration of Taq enzyme was 0.2 U μl^{-1} , which was twice of that used in the conventional approaches. In addition, the flow rate of 41.2 $\mu\text{l min}^{-1}$, corresponding to residence times of 6 s in the denaturizing zone, 6 s in the annealing zone, and 13 s in the elongation zone, was chosen in this experiment for obtaining the desired production and time of amplification. Figure 5a shows the on-line fluorescence detection results of the amplified 327 bp sequence amplified under the serially diluted cDNA from NVs RNA, whereas Fig. 5b shows the gel electrophoresis results. The tenfold serial dilution of cDNA is estimated to be from 5×10^8 to 5×10^2 copies μl^{-1} of the corresponding RNA concentrations. As seen from Fig. 5, the yields of PCR products are reduced with decreasing the corresponding RNA concentrations from 5×10^8 to 5×10^2 copies μl^{-1} . The

Table 2 Comparison of different spiral-channel continuous-flow PCR microfluidics for DNA analysis

Flow rate	Residence time		Amplification time (min)	Cycle number	Cycle time (s)	Residence time			Tube size, i.d. (μm)/o.d. (μm)	Amplicon length (bp)	Method of segmented flow	Reference
	Linear flow rate (mm s^{-1})	Volume flow rate ($\mu\text{l min}^{-1}$)				Denaturation (s)	Annealing (s)	Extension (s)				
6.36 ^a		3.0	8.5 ^a	33	15 ^a	4 ^a	4 ^a	4 ^a	100/240	323	Gas-liquid systems	Park et al. (2003)
9.78 ^a		18.42 ^a	23 ^a	30	45	11 ^a	11 ^a	23 ^a	200/400	79	Liquid-liquid systems	Curcio and Roeraade (2003)
N/A		50	34 ^a	42	48 ^a	6	9	15	N/A	292	Liquid-liquid systems	Hartung et al. (2009)
1		30.14 ^a	70 ^a	35	120 ^a	30 ^a	30 ^a	60 ^a	800/N/A	572	Liquid-liquid systems	Dorfman et al. (2005)
1		27.2 ^a	70 ^a	35	120 ^a	30 ^a	30 ^a	60 ^a	760/N/A	572	Liquid-liquid systems	Chabert et al. (2006)
0.4 ^a		6	210 ^a	40	300 ^a	150 ^a	150 ^{a, b}		550/1070	N/A	Liquid-liquid systems	Markey et al. (2010)
7.5		88.3	10	40	15	3	3	6	500/900	327	Gas-liquid systems	This work

^a The data were calculated by the authors^b 150 s was the total residence time of the annealing and extension processes**Fig. 5** Analysis of the products from different amounts of cDNA amplified by the continuous-flow PCR. **a** Fluorescence detection of PCR products. **b** Gel electrophoresis analysis of PCR products. Lane M DL 2000 Marker. Lane 1 the positive-control PCR product from the conventional PCR machine (a commercial Mastercycler gradient PCR machine). Lanes 2–8 PCR products from tenfold serial dilution cDNA, which is estimated to be from 5×10^8 to 5×10^2 copies μl^{-1} of the corresponding RNA concentrations, on the continuous-flow PCR at a flow rates of $41.2 \mu\text{l min}^{-1}$. Lane 9 the negative-control PCR, PCR mixture solution with no cDNA sample run at the flow rate of $58.9 \mu\text{l min}^{-1}$

lowest corresponding RNA concentration that could be visibly detected by on-line fluorescence detection and agarose gel electrophoresis is up to 5×10^3 copies μl^{-1} (lane 7 in Fig. 5b).

3.3 Evaluation of the RT reaction

For RT-PCR, a RT process is typically needed before PCR. Thus, the cDNA, which is used as a DNA template during PCR, is synthesized from RNA by the RT reaction. In this study, the RT reaction of RNA samples was carried out within the columnar reactor, where a reaction temperature of 42°C and a residence time of 45 min were programmed when a flow rate of $23.6 \mu\text{l min}^{-1}$ was used. To investigate

the possibility of rapid RT reactor, a flow rate of $35.4 \mu\text{l min}^{-1}$ was also used in the experiments, which corresponded to a residence time of about 30 min. After the continuous-flow RT process, the cDNA was amplified on the commercial Mastercycler gradient PCR machine (cPCR), and the quality of the obtained products was analyzed by gel electrophoresis. As shown in Fig. 6, successful cDNA synthesis from NVs RNA samples was obtained using the developed miniaturized RT device. The experiments results shown in the first and second lanes of Fig. 6 correspond to the 327 bp RT-PCR products obtained using the conventional PCR machine, with the conventional RT (cRT) reaction time of 45 and 30 min, respectively. Meanwhile, the fourth and final lanes of Fig. 6 correspond to the products amplified from the cDNA synthesized on the continuous-flow RT reactor (μRT) with the residence time of 30 and 45 min, respectively. Note that the signals from the μRT are comparable with the signals obtained using the conventional machine. In other words, the reverse transcription capability of micro device is equivalent to that of the commercial device.

In Fig. 7, the RT step of the RNA and the PCR step of the cDNA were crosswise accomplished in the micro-reactors and in a conventional cyclor. The results showed a successful two-step continuous-flow RT-PCR reaction ($\mu\text{RT}-\mu\text{PCR}$) based on RVs RNA samples on the presented device (lane 2 in Fig. 7). The experimental result of the cDNA synthesized from μRT and then amplified using cPCR ($\mu\text{RT}-\text{cPCR}$) was shown in lane 1 of Fig. 7. Meanwhile, the third and forth lanes of Fig. 7 were the amplification results with μPCR (cRT- μPCR) (lane 3 in Fig. 7) and cPCR (cRT-cPCR) (lane 4 in Fig. 7) from the cDNA synthesized using cRT. Importantly, it can be seen from Fig. 7 that the specificity of the reactions performed on the

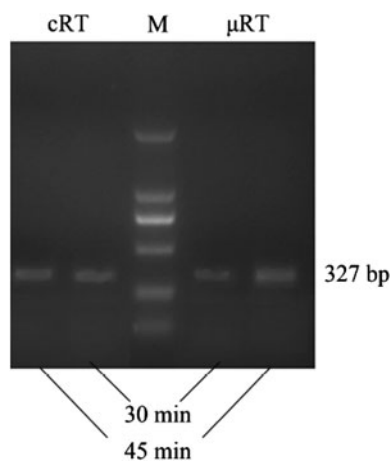


Fig. 6 Evaluation of the cDNA synthesis on the continuous-flow RT reactor (μRT) compared with the conventional thermocycler (cRT). The reaction times were 45 min (the first and final lanes) and 30 min (the second and forth lanes), respectively

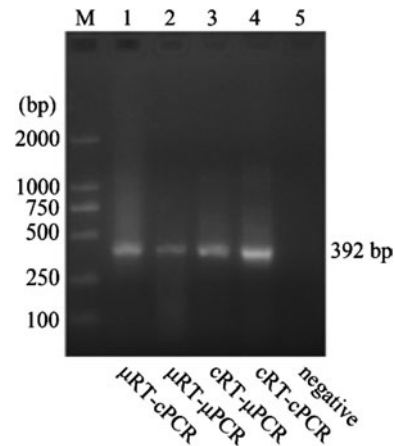


Fig. 7 Gel electrophoresis analysis of two-step RT-PCR parallel performed in the micro-reactors and in a conventional thermocycler. Lane M DL 2000 Marker. Lane 1 the cDNA was synthesized from continuous-flow RT reactor (μRT) and then amplified using the conventional PCR machine (cPCR) ($\mu\text{RT}-\text{cPCR}$). Lane 2 a two-step RT-PCR accomplished using the presented device ($\mu\text{RT}-\mu\text{PCR}$). Lane 3 the cDNA was synthesized with the conventional thermocycler (cRT) and then amplified using continuous-flow PCR reactor (μPCR) (cRT- μPCR). Lane 4 a two-step RT-PCR accomplished using the conventional PCR machine (cRT-cPCR). Lane 5 the negative-control two-step $\mu\text{RT}-\mu\text{PCR}$, reaction mixture solution with no RNA sample

microfluidic device was higher than on the conventional apparatus, although the product yield was less than the latter. This phenomenon, similar to our previous works (Li et al. 2009), may be attributed to the fact that the ramping rates of the microfluidic devices are higher than those of the conventional apparatus, and as a result the possibility that the nonspecific PCR products derive from false priming is decreased.

3.4 Integrated continuous-flow RT-PCR with fluorescence detection for identification of pathogenic NVs and RVs

It is of great important that a one-step RT-PCR reaction based on labile RNA samples can be performed in the continuous-flow micro-reactors ($\mu\text{RT}-\text{PCR}$). Figure 8 shows the experiments with $\mu\text{RT}-\text{PCR}$ for the detection of NVs and RVs (lanes 2 and 3 in Fig. 8b), comparable to the commercial thermocycler (cRT-PCR) (lanes 1 and 4 in Fig. 8b). Figure 8a shows the on-line fluorescence detection results, whereas Fig. 8b shows the corresponding gel electrophoresis results. The results demonstrate that the performance of the developed miniature RT-PCR system is superior to that of the conventional PCR machine with respect to rapidity and integration. In addition, it is worth noting that the specificity of the reactions performed using $\mu\text{RT}-\text{PCR}$ (lanes 5 in Fig. 8b) is also higher than cRT-PCR (lanes 4 in Fig. 8b), although the product yield is less than the latter. This phenomenon is similar to that within the

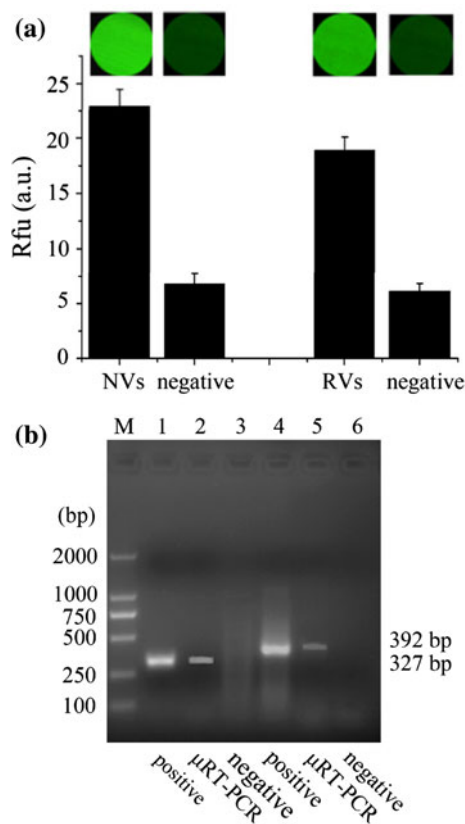


Fig. 8 Results of the identification of pathogenic NVs and RVs using a one-step RT-PCR reaction based on RNA samples in the continuous-flow micro-reactors (μ RT-PCR). **a** On-line fluorescence detection of μ RT-PCR products. **b** Gel electrophoresis analysis of μ RT-PCR products. Lane M DL 2000 Marker. Lanes 1 and 4 the positive-control one-step RT-PCR products from the conventional PCR machine (cRT-PCR) for the detection of NVs and RVs, respectively. Lanes 2 and 5 the results of the μ RT-PCR for the detection of NVs and RVs, respectively. Lanes 3 and 6 the negative-control results of the μ RT-PCR for the detection of NVs and RVs, respectively

two-step RT-PCR reaction (Fig. 7), and the possible reasons have been discussed above.

3.5 Sensitivity of continuous-flow RT-PCR assay for RVs diagnostics

For practical applications such as clinical diagnosis, it is essential to determine the sensitivity of the one-step continuous-flow RT-PCR assay. The LOD for the developed system was tested with RVs RNA templates, where serial dilutions of RNA (tenfold dilutions from 6.4×10^8 to 6.4×10^2 copies μl^{-1}) were used. As shown in Fig. 9, the yields of RT-PCR products are decreased with reduction of RNA concentrations, and the LOD of RVs RNA is 6.4×10^4 copies μl^{-1} (lane 6 in Fig. 9b). The comparison between Figs. 5 and 9 shows that the one primary

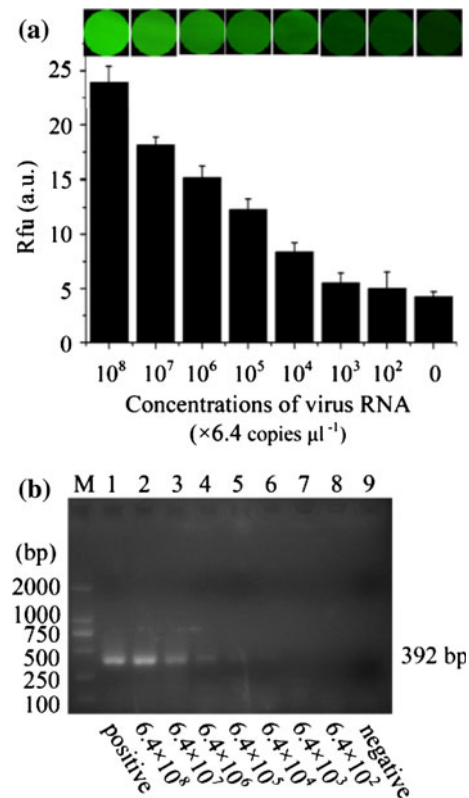


Fig. 9 Analysis of the products amplified by one-step continuous-flow μ RT-PCR from various concentrations of input virus RNA. **a** Fluorescence intensity of μ RT-PCR products. **b** Gel electrophoresis analysis of the products. Lane M DL 2000 Marker. Lane 1 the positive-control μ RT-PCR product from the conventional PCR machine (a commercial Mastercycler gradient PCR machine). Lanes 2–8 μ RT-PCR products from tenfold serial dilution RNA, which concentrations are estimated to be from 6.4×10^8 to 6.4×10^2 copies μl^{-1} . Lane 9 the negative-control result of μ RT-PCR

drawback to the present one-step RT-PCR process is the lower amplification efficiency. It is conceivable that the reaction efficiency of the microfluidic device could be enhanced if a single reaction buffer, which is suitable for both the RT and PCR steps, was used in the experiments. In this study, we used the PCR buffer for the one-step RT-PCR reactions, which may reduce the reaction efficiency due to the inconsistent buffer conditions for reverse transcriptase and Taq polymerase.

3.6 Segmented-flow RT-PCR for simultaneous detection of pathogenic NVs and RVs

In the conventional RT-PCR approaches, multiplex RT-PCR has attracted much attention and been widely applied in clinical services owing to the reduction in labor and time. For continuous-flow PCR, one of the important superiorities is that it provides the possibility of performing successive DNA amplification by using a continuous

segmented flow of different PCR mixtures containing different DNA target samples. This format of amplification can save time and simplify the operation to a large extent. During recent years, some researchers have developed the successive amplification of different PCR mixtures and the approaches of contamination-free amplification in a continuous-flow format (Obeid et al. 2003; Obeid and Christopoulos 2003; Park et al. 2003; Curcio and Roeraade 2003; Dorfman et al. 2005; Chabert et al. 2006).

In this study, we used the method similar to the work of Park et al. (2003) to avoid the cross-contamination from successive RT-PCR with different samples. To cleanse the carryover from the preceding segment to the following one, we interposed $1 \times$ PCR buffer containing $0.2 \times$ BPB buffer between each segment. The BPB buffer is widely used in loading DNA samples on electrophoresis gels, and DNA molecules would dissolve into it very well. Moreover, it is blue, and each sample segment is easily located. Figure 10a illustrates the segmented-flow mode of continuous RT-PCR amplification of different RNA samples. Figures 10b, c display the results of successive RT-PCR amplification for detecting NVs and RVs contemporaneously. Here, it should be accentuated that there are also small amounts of amplification products in BPB buffers

(lanes 2 and 6 in Fig. 10c), but no products of amplification were found with the negative controls (lanes 3 and 7 in Fig. 10c). Therefore, the practical results from our experiments showed that the cleaning method was able to reduce the RT-PCR residue between different samples, which may result from adsorption of analyte or reagents, and surface imperfections of the capillary.

3.7 Comparison of different continuous-flow PCR devices for DNA and/or RNA analysis

Over the last several years, the development of the functional integration of RT and PCR has attracted great interest, and has witnessed steady advances. In general, the microfluidic RT-PCR devices can be classified as microchamber stationary RT-PCR and continuous-flow RT-PCR. Compare with the former, continuous-flow RT-PCR has the flexibility to change the reaction speed by utilizing the “time–space conversion” concept. However, up to now, only a few examples of continuous-flow RT-PCR were demonstrated. Several typical results are compared and listed in Table 3. To the authors’ thinking, the continuous-flow RT-PCR microfluidics may be divided into two structural styles: serpentine channel and spiral channel. Obeid et al. (2003)

Fig. 10 Results of the simultaneous detection of pathogenic NVs and RVs using a one-step segmented-flow RT-PCR reaction based on RNA samples. **a** Segmented-flow mode of continuous-flow RT-PCR for different RNA samples. **b** On-line fluorescence intensity detection of products. **c** Gel electrophoresis analysis of products. Lane M DL 2000 Marker. Lanes 1 and 5 the results of the μ RT-PCR for the detection of RVs and NVs, respectively. Lanes 2, 4, and, 7 BPB buffer. Lanes 3 and 5 the negative-control results of the μ RT-PCR for the detection of RVs and NVs, respectively

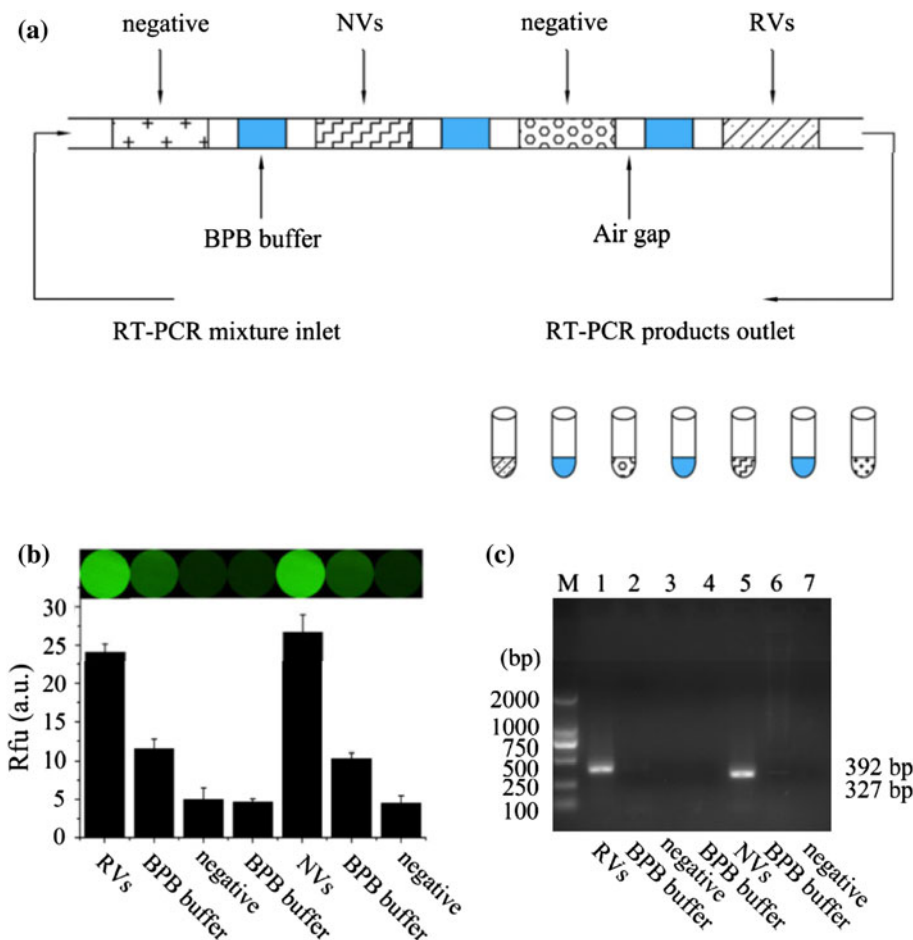


Table 3 Comparison of similar miniaturized PCR devices for nucleic acid analysis

Structural style	Channel material	RT	Detection method	Target RNA	Reference
Serpentine channel	Glass	Yes	Off-line agarose gel electrophoresis	1 kb fragment synthesized by in vitro transcription of prostate-specific antigen (PSA)	Obeid et al. (2003)
Serpentine channel	SU-8	Yes	Off-line agarose gel electrophoresis	Tumor viruses	Tsai and Sue (2006)
Serpentine channel	Glass	Yes	Off-line agarose gel electrophoresis	RNA from human papilloma virus type 16 (HPV 16)	Felbel et al. (2008)
Serpentine channel	Glass	Yes	On-line end-point LIF	1 kb fragment synthesized by in vitro transcription of PSA	Obeid and Christopoulos (2003)
Spiral channel	FEP tube	Yes	Off-line agarose gel electrophoresis and southern blot	RNA from HPV 16 positive SiHa cells and mRNA from measles viruses	Hartung et al. (2009)
Spiral channel	PTFE tubing	No	N/A	N/A	Markey et al. (2010)
Spiral channel	Fused-silica capillary	No	Off-line agarose gel electrophoresis	N/A	Park et al. (2003)
Spiral channel	PFA capillary	No	Off-line agarose gel electrophoresis	N/A	Dorfman et al. (2005)
Spiral channel	PFA capillary	No	On-line end-point LIF	N/A	Chabert et al. (2006)
Spiral channel	Teflon tube	No	On-line end-point LIF	N/A	Curcio and Roeraade (2003)
Spiral channel	PTFE capillary	Yes	On-line end-point fluorescence detection	RNA from Noroviruses and Rotaviruses	This work

developed a microfabricated glass chip for the functional integration of RT and PCR in a serpentine-channel continuous-flow mode. Similar studies were also performed by Tsai and Sue (2006) and Felbel et al. (2008) using the serpentine-channel continuous-flow RT-PCR system. However, the detection method was off-line agarose gel electrophoresis, which was time-consuming and labor-intensive. Another analysis method of the amplified PCR products is fluorescence scan after PCR test (Xiang et al. 2007). For example, Obeid and Christopoulos (2003) combined the continuous-flow RNA amplification with the laser-induced fluorescence (LIF) detection on a single chip. However, for serpentine-channel continuous-flow RT-PCR chips, parallelization is not easily realized as it complicates the chip architecture and most likely increases the chip footprint. Importantly, within these RT-PCR chips, the PCR temperature zones are linearly arranged and are easy to establish a smooth temperature gradient, which is denaturation temperature → extension temperature → annealing temperature. In this instance, however, the melted single-stranded DNA is very likely to form double strands with the template strands or their complementary fragments when passing the extension zone, which compromises the PCR efficiency.

In order to circumvent this problem, another approach of continuous-flow PCR is exploited, which was a helical arrangement of the reaction tube in a columnar reactor to generate the sequence of denaturation, annealing, and

extension (Park et al. 2003; Curcio and Roeraade 2003; Dorfman et al. 2005; Chabert et al. 2006; Markey et al. 2010). To our knowledge, Hartung et al. (2009) first established a fast continuous-flow RT-PCR process consisting of two columnar reactors for thermostating the different reaction zones of the RT process and the amplification. However, one shortcoming of their work is that it still used off-line detection method for the diagnosis of pathogenic viruses. Although a miniaturized fluorescence detector was used to measure the fluorescence intensity of the single fluid segments inside the reaction tube, it only in situ detected double-stranded DNA in the experiments, and was not used for on-line detection of RT-PCR-based RNA viruses. When compared to the work of Hartung et al. (2009), the continuous-flow RT-PCR proposed in this article realized the on-line end-point fluorescence detection for rapid diagnosis of NVs and RVs. In addition, it can be seen from Table 2 that the currently presented PCR process speed demonstrated in this work is not slower, and even faster in comparison with other reports, which also used spiral-channel-based continuous-flow PCR devices.

4 Conclusions

A microfluidic system for continuous-flow RT-PCR reactions with on-line fluorescence detection has been developed for fast identification of RNA-based viruses, namely

NVs and RVs, which are now widely known to be the most common etiological agents of nonbacterial acute gastroenteritis causing numerous outbreaks worldwide. The bath refrigerating presents the proposed miniature system a better temperature control and uniformity for a more compact structural design. The developed microfluidic system not only overcomes the thermal cross-talk effects of radiation and/or conduction but also utilizes fluorescence microscopy to realize the on-line product detection. Up to now, the amplification products of most microfluidic RT-PCR (Felbel et al. 2008; Hartung et al. 2009; Lee et al. 2008; Liao et al. 2005; Lien et al. 2007; Lien et al. 2009; Tsai and Sue 2006) have been analyzed by agarose gel electrophoresis and ethidium bromide staining, which is time-consuming and labor-intensive. Therefore, our current efforts are focused on the on-line fluorescence detection, which offers several obvious advantages. First, compared with conventional gel electrophoresis that requires about 30 min for gel casting, the on-line detection system does not require gel preparation. Second, the products detection is completed within 1 min, whereas gel electrophoresis generally requires about 30 min running time. Third, the detection volumes in this system can be decreased to less than 1 μl , whereas gel electrophoresis usually requires several microliters of amplification products. The identification of NVs and RVs could be successfully completed within less than 1 h on this compact, spiral-channel-based, continuous-flow RT-PCR microfluidics, and thus the whole microfluidic reaction process was much faster than that of the conventional RT-PCR process. In addition, the LOD of the RVs RNA concentration was estimated to be 6.4×10^4 copies μl^{-1} . However, the common drawbacks, such as adsorption of the reagents to the channel surface (Zhang et al. 2006), being prone to evaporation of the sample solution and formation of gas bubbles (Zhang and Xing 2010a), the requirement of precise temperature control are also the challenging issues to be solved for increasingly popularity of microfluidic RT-PCR in the future. Despite these obstacles, we believe that the microfluidic RT-PCR and on-line fluorescence detection described here holds great potential for the rapid detection of RNA-based viruses in a convenient platform.

Acknowledgments This research is supported by the National Natural Science Foundation of China (30700155), the Key Program of NSFC-Guangdong Joint Funds of China (U0931005), the Program for Changjiang Scholars and Innovative Research Team in University (IRT0829), and the National High Technology Research and Development Program of China (863 Program) (2007AA10Z204). We are grateful to Guangdong provincial center for diseases control and prevention (GDCDC, Guangzhou, China) and Guangzhou overseas Chinese hospital (The first affiliated hospital of Jinan university, Guangzhou, China) for their offers of the viruses RNA samples.

References

- Atmar RL, Estes MK (2001) Diagnosis of noncultivable gastroenteritis viruses, the human caliciviruses. *Clin Microbiol Rev* 14:15–37
- Becker KM, Moe CL, Southwick KL, MacCormack JN (2000) Transmission of Norwalk virus during football game. *N Engl J Med* 343:1223–1227
- Beer NR, Hindson BJ, Wheeler EK, Hall SB, Rose KA, Kennedy IM, Colston BW (2007) On-chip, real-time, single-copy polymerase chain reaction in picoliter droplets. *Anal Chem* 79:8471–8475
- Beer NR, Wheeler EK, Lee-Houghton L, Watkins N, Nasarabadi S, Hebert N, Leung P, Arnold DW, Bailey CG, Colston BW (2008) On-chip single-copy real-time reverse-transcription PCR in isolated picoliter droplets. *Anal Chem* 80:1854–1858
- Belgrader P, Elkin CJ, Brown SB, Nasarabadi SN, Langlois RG, Milanovich FP, Colston BW, Marshall GD (2003) A reusable flow-through polymerase chain reaction instrument for the continuous monitoring of infectious biological agents. *Anal Chem* 75:3446–3450
- Chabert M, Dorfman KD, de Cremoux P, Roeraade J, Viovy JL (2006) Automated microdroplet platform for sample manipulation and polymerase chain reaction. *Anal Chem* 78:7722–7728
- Curcio M, Roeraade J (2003) Continuous segmented-flow polymerase chain reaction for high-throughput miniaturized DNA amplification. *Anal Chem* 75:1–7
- Dorfman KD, Chabert M, Codarbox JH, Rousseau G, de Cremoux P, Viovy JL (2005) Contamination-free continuous flow microfluidic polymerase chain reaction for quantitative and clinical applications. *Anal Chem* 77:3700–3704
- Felbel J, Reichert A, Kielpinski M, Urban M, Henkel T, Häfner N, Dürst M, Weber J (2008) Reverse transcription-polymerase chain reaction (RT-PCR) in flow-through micro-reactors: thermal and fluidic concepts. *Chem Eng J* 135S:S298–S302
- Gouvea V, Allen JR, Glass RI, Woods P, Taniguchi KC, Lark HF et al (1990) Polymerase chain reaction amplification and typing of RV nucleic acid from stool specimens. *J Clin Microbiol* 28:276–282
- Hartung R, Brösing A, Szczepankiewicz G, Liebert U, Häfner N, Dürst M, Felbel J, Lassner D, Köhler JM (2009) Application of an asymmetric helical tube reactor for fast identification of gene transcripts of pathogenic viruses by micro flow-through PCR. *Biomed Microdevices* 11:685–692
- Hoang VN, Kaigala GV, Atrazhev A, Pilarski LM, Backhouse CJ (2008) Strategies for enhancing the speed and integration of microchip genetic amplification. *Electrophoresis* 29:4684–4694
- Hsieh TM, Luo CH, Wang JH, Lin JL, Lien KY, Lee GB (2009) A two-dimensional, self-compensated, microthermal cyclor for one-step reverse transcription polymerase chain reaction applications. *Microfluid Nanofluid* 6:797–809
- Huang FC, Liao CS, Lee GB (2006) An integrated microfluidic chip for DNA/RNA amplification, electrophoresis separation and on-line optical detection. *Electrophoresis* 27:3297–3305
- Kaigala GV, Hoang VN, Stickel A, Lauzon J, Manage D, Pilarski LM, Backhouse CJ (2008) An inexpensive and portable microchip-based platform for integrated RT-PCR and capillary electrophoresis. *Analyst* 133:331–338
- Kiss MM, Ortoleva-Donnelly L, Beer NR, Warner J, Bailey CG, Colston BW, Rothberg JM, Link DR, Leamon JH (2008) High-throughput quantitative polymerase chain reaction in picoliter droplets. *Anal Chem* 80:8975–8981
- Koopmans M, De Bruin E, Vennema H (2002) Rational optimization of generic primers used for Norwalk-like virus detection by transcription polymerase chain reaction. *J Clin Methods* 25:233–236

- Kopp MU, de Mello AJ, Manz A (1998) Chemical amplification: continuous-flow PCR on a chip. *Science* 280:1046–1048
- Kou XX, Wu QP, Wang DP, Zhang JM (2008) Simultaneous detection of norovirus and rotavirus in oysters by multiplex RT-PCR. *Food Control* 19:722–726
- Lee SH, Kim SW, Kang JY, Ahn CH (2008) A polymer lab-on-chip for reverse transcription (RT)-PCR based point-of-care clinical diagnostics. *Lab chip* 8:2121–2127
- Li YY, Xing D, Zhang CS (2009) Rapid detection of genetically modified organisms (GMOs) on a continuous-flow PCR microfluidics. *Anal Biochem* 385:42–49
- Liao CS, Lee GB, Liu HS, Hsieh TM, Luo CH (2005) Miniature RT-PCR system for diagnosis of RNA-based viruses. *Nucleic Acids Res* 33:e156
- Lien KY, Lee SH, Tsai TJ, Chen TY, Lee GB (2009) A microfluidic-based system using reverse transcription polymerase chain reactions for rapid detection of aquaculture diseases. *Microfluid Nanofluid* 7:795–806
- Liu J, Enzelberger M, Quake S (2002) A nanoliter rotary device for polymerase chain reaction. *Electrophoresis* 23:1531–1536
- Marcus JS, Anderson WF, Quake SR (2006a) Microfluidic single-cell mRNA isolation and analysis. *Anal Chem* 78:3084–3089
- Marcus JS, Anderson WF, Quake SR (2006b) Parallel picoliter RT-PCR assays using microfluidics. *Anal Chem* 78:956–958
- Markey AL, Mohr S, Day PJR (2010) High-throughput droplet PCR. *Methods* 50:277–281
- Marks PJ, Vipond IB, Regan FM, Wedgwood K, Fey RE, Caul EO (2003) A school outbreak of Norwalk-like virus: evidence for airborne transmission. *Epidemiol Infect* 131:727–736
- Medici MC, Martinelli M, Ruggeri FM, Abelli LA, Bosco S, Arcangeletti MC, Pinardi F, Conto FD, Calderaro A, Chezzi C, Dettori G (2005) Broadly reactive nested reverse transcription-PCR using an internal RNA standard control for detection of noroviruses in stool samples. *J Clin Microbiol* 43:3772–3778
- Nakano H, Matsuda K, Yohda M, Nagamune T, Endo I, Yamane T (1994) High speed polymerase chain reaction in constant flow. *Biosci Biotech Biochem* 58:349–352
- Northrup MA, Ching MT, White RM, Watson RT (1993) DNA amplification in a microfabricated reaction chamber. In: *Proceeding of the 7th international conference on solid state sensors and actuators, Yokohama, Japan*, pp 924–926
- Obeid PJ, Christopoulos TK (2003) Continuous-flow DNA and RNA amplification chip combined with laser-induced fluorescence detection. *Anal Chim Acta* 494:1–9
- Obeid PJ, Christopoulos TK (2004) Microfabricated systems for nucleic acid analysis. *Crit Rev Clin Lab Sci* 41:429–465
- Obeid PJ, Christopoulos TK, Crabtree HJ, Backhouse CJ (2003) Microfabricated device for DNA and RNA amplification by continuous-flow polymerase chain reaction and reverse transcription-polymerase chain reaction with cycle number selection. *Anal Chem* 75:288–295
- Ottesen EA, Hong JW, Quake SR, Leadbetter JR (2006) Microfluidic digital PCR enables multigene analysis of individual environmental bacteria. *Science* 314:1464–1467
- Park N, Kim S, Hahn JH (2003) Cylindrical compact thermal-cycling device for continuous-flow polymerase chain reaction. *Anal Chem* 75:6029–6033
- Prakash R, Kaler KVIS (2007) An integrated genetic analysis microfluidic platform with valves and a PCR chip reusability method to avoid contamination. *Microfluid Nanofluid* 3:177–187
- Prakash AR, Amrein M, Kaler KVIS (2008a) Characteristics and impact of *Taq* enzyme adsorption on surfaces in microfluidic devices. *Microfluid Nanofluid* 4:295–305
- Prakash AR, De la Rosa C, Fox JD, Kaler KVIS (2008b) Identification of respiratory pathogen *Bordetella pertussis* using integrated microfluidic chip technology. *Microfluid Nanofluid* 4:451–456
- Saiki RK, Scharf F, Faloona F, Mullis KB, Horn GT, Erlich HA, Arnheim N (1985) Enzymatic amplification of beta-globin genomic sequences and restriction site analysis for diagnosis of sickle cell anemia. *Science* 230:1350–1354
- Trantakis IA, Fakis M, Tragoulias SS, Christopoulos TK, Persephonis P, Glanetas V, Ioannou P (2010) Ultrafast fluorescence dynamics of Sybr Green I/DNA complexes. *Chem Phys Lett* 485:187–190
- Tsai NC, Sue CY (2006) SU-8 based continuous-flow RT-PCR biochips under high-precision temperature control. *Biosens Bioelectron* 22:313–317
- VanDijken J, Kaigala GV, Lauzon J, Atrazhev A, Adamia S, Taylor BJ, Reiman T, Belch AR, Backhouse CJ, Pilarski LM (2007) Microfluidic chips for detecting the t(4; 14) translocation and monitoring disease during treatment using reverse transcriptase-polymerase chain reaction analysis of IgH-MMSET hybrid transcripts. *J Mol Diagn* 9:358–367
- Wang HY, Zhang CS, Li YY (2009) Rapid detection of tobacco mosaic virus from crude samples on an oscillatory-flow reverse transcription polymerase chain reaction microfluidics. *Chin J Anal Chem* 37:1286–1290
- Xiang Q, Xu B, Li D (2007) Miniature real time PCR on chip with multi-channel fiber optical fluorescence detection module. *Biomed Microdevices* 9:443–449
- Zhang CS, Xing D (2007) Miniaturized PCR chips for nucleic acid amplification and analysis: latest advances and future trends. *Nucleic Acids Res* 35:4223–4237
- Zhang CS, Xing D (2010a) Decreasing microfluidic evaporation loss using the HMDL method: open systems for nucleic acid amplification and analysis. *Microfluid Nanofluid* 9:17–30
- Zhang CS, Xing D (2010b) Microfluidic gradient PCR (MG-PCR): a new method for microfluidic DNA amplification. *Biomed Microdevices* 12:1–12
- Zhang CS, Xu JL, Zheng WL (2006) PCR microfluidic devices for DNA amplification. *Biotechnol Adv* 24:243–284
- Zhang CS, Xing D, Li YY (2007) Micropumps, microvalves, and micromixers within PCR microfluidic chips: advances and trends. *Biotechnol Adv* 25:483–514